Optics Communications 363 (2016) 91–96

Contents lists available at ScienceDirect

Optics Communications

journal homepage: www.elsevier.com/locate/optcom

Discharge processes of UV pre-ionized electric-discharge pulsed DF laser

Qikun Pan*, Jijiang Xie, Chunlei Shao, Chunrui Wang, Mingzhen Shao, Jin Guo

State Key Laboratory of Laser Interaction with Matter, Changchun Institute of Optics, Fine Mechanics and Physics, Chinese Academy of Sciences, Changchun 130033, China

ARTICLE INFO

Article history:
Received 27 August 2015
Received in revised form
31 October 2015
Accepted 3 November 2015
Available online 14 November 2015

Keywords:
Non-chain DF laser
Gas discharge
Numerical simulation
Ultraviolet pre-ionization

ABSTRACT

The discharge processes of ultraviolet (UV) pre-ionized electric-discharge pulsed DF laser operating with a SF_6–D_2 gas mixture are studied. A mathematical model based on continuity equation of electrons and Kirchhoff equations for discharge circuit is established to describe the discharge processes. Voltage and current waveforms of main discharge and voltage waveforms of pre-ionization are solved numerically utilizing the model. The calculations correctly display some physical processes, such as the delay time between pre-ionization and main discharge, breakdown of the main electrode and self-sustained volume discharge (SSVD). The results of theory are consistent with the experiments, which are performed in our non-chain pulsed DF laser. Then the delay inductance and peak capacitance are researched to analyze their influences on discharge processes, and the circuit parameters of DF laser are given which is useful to improve the discharge stability.

1. Introduction

Electric discharge non-chain pulsed HF/DF lasers have attracted much attention in the field of high power medium wave infrared lasers, which have significant applications in many fields such as spectroscopy, laser radar transmitters, laser ranging, atmospheric monitoring, military, etc. [1–6]. Usually, these lasers use strong electronegative SF_6 as F atoms donor, which makes it difficult to develop uniform and stable discharge in gas mixture, especially with a bigger discharge gap. In order to obtain stable SSVD in mixtures of SF_6, many kinds of discharge technologies were used. Rickwood obtained stable discharge with semiconductor pre-ionizer Electric discharge technology, whose maximum discharge gap was 1.2 cm and cathode area was $50 \times 0.9\ \mathrm{cm}^2$ [7]. Scott presented an X-ray pre-ionized self-sustained discharge DF/HF laser, whose maximum stable discharge gap was 2.4 cm and cathode area was $45 \times 2\ \mathrm{cm}^2$ [8]. Brunet reported photo-triggered discharge, which pre-ionization pulse was applied when the voltage across the electrodes was well above the steady-state breakdown voltage, obtaining a uniform discharge in the region with gap of 3.5 cm, length of 45 cm and width of 8 cm [9]. Apollonov introduced a self-initiated volume discharge (SIVD), which the cathode surface possessed of small-scale (50 μm) non-uniformities and the discharge characteristics was independent of pre-ionization. Based on this new discharge technology, the stable discharge gap reached 27 cm with the cathode area of $100 \times 20\ \mathrm{cm}^2$ [10]. In our lab a stable SSVD is obtained with spark pin UV pre-ionization discharge technology, and the output energy was 4.95 J with pulse duration of 149 ns [11].

The discharge stability and deposited energy must be further enhanced in order to obtain preferable output performances, which would require detailed experimental study on circuit parameters of DF laser. And the theoretical model of discharge circuit is helpful to understand the discharge processes, predict optimum circuit parameters and explain the experimental results, all of which have extremely vital significance for experimental study.

In this paper, the circuit characters of non-chain pulsed DF laser, initiated by UV pre-ionization electric-discharge, are researched theoretically and experimentally. The aim of our work is to study in more detail the SSVD development in time and to obtain optimum circuit parameters that govern the discharge processes.

2. Physical processes of discharge in DF laser

2.1. Discharge circuit

The LC inversion circuit used in our non-chain pulse DF laser for investigating the processes of discharge is presented schematically in Fig. 1. C_1 and C_2 are storage capacitances of main

* Correspondence to: Changchun Institute of Optics, Fine Mechanics and Physics, Chinese Academy of Sciences, Changchun 130033, China.
E-mail address: panqikun2005@163.com (Q. Pan).

http://dx.doi.org/10.1016/j.optcom.2015.11.004
0030-4018/

electrodes and pre-ionization electrodes. C_3 is peaking capacitance and L is delay inductance. L_1, L_2 are charging inductances and SG is rotary spark switch. HV and TV are high voltage source and trigger source respectively. A, B are the voltage test points of main discharge and pre-ionization discharge respectively. Plane electrodes as main electrodes were used in the laser system, and the spark pins as pre-ionization electrodes were set both sides of the electrodes symmetrically, as shown in Fig. 2. The discharge is formed between plane electrodes of size 120 cm × 4 cm, which are spaced by a 4 cm gap.

Working processes of LC inversion circuit is described as follows. Firstly, HV charge to C_1 and C_2 through L_1 and L_2 respectively. Secondly, under the control of TV, the circuit is reversed after the breakdown of SG switch. However, breakdown of main electrodes cannot be realized due to strong electronegativity of SF_6, which is responsible for the high impedance of gas mixture, and C_1 will charge to C_3 at the moment. The gap between the spark pins is small and the electric field is more concentrated at the pinpoint, so the pre-ionization electrodes generate spark discharge with the breakdown of SG. Intense UV radiation generated from spark discharge passes through the gap and forms photoionization, which produces a large quantity of initial electrons and decrease impedance of gas mixture. Lastly, under the effect of UV pre-ionization, C_3 will discharge to the main electrodes and initiate stable SSVD in the gas mixture.

2.2. Calculation model of discharge circuit

The equivalent circuit of LC inversion circuit is shown in Fig. 3. The resistance of SG (R_{SG}) is equivalent to a variable resistance. Before breakdown of SG switch, the value of R_{SG} is infinitely great, and whose branch circuit is equivalent to open. Contrarily, with the breakdown of SG, the value of R_{SG} rapidly goes to infinitely little and the branch circuit is equivalent to short. The reference directions of current for each branch circuits are marked in Fig. 3.

Using the circuit equations of Kirchhoff, some equations that can describe the relation between circuit parameters with time have been given by the following equations:

$$\frac{du_1}{dt} = -\frac{i_L}{C_1} + \frac{i_{L2}}{C_1} + \frac{u_d - u_1 + u_2}{R_{pre} \cdot C_1} \quad (1)$$

$$\frac{du_2}{dt} = -\frac{i_{L2}}{C_2} - \frac{u_d - u_1 + u_2}{R_{pre} \cdot C_2} \quad (2)$$

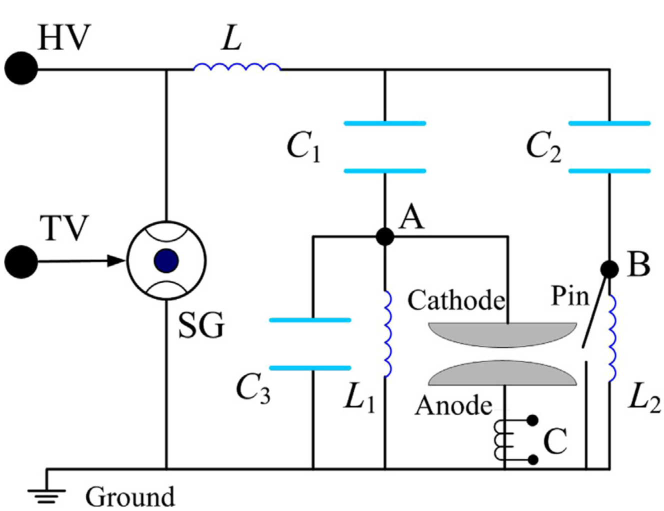

Fig. 1. Circuit diagram of LC inversion circuit.

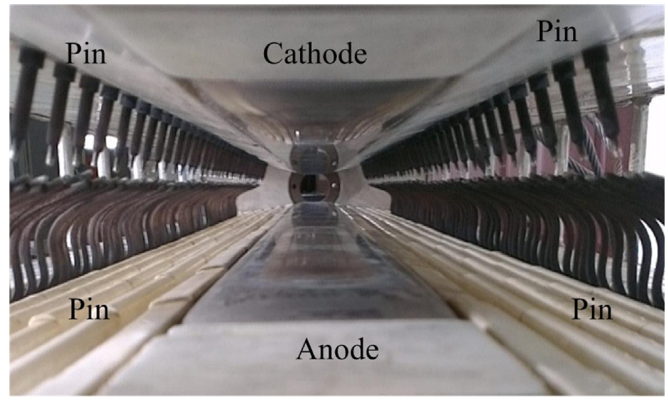

Fig. 2. Photograph of plane electrodes and spark pins.

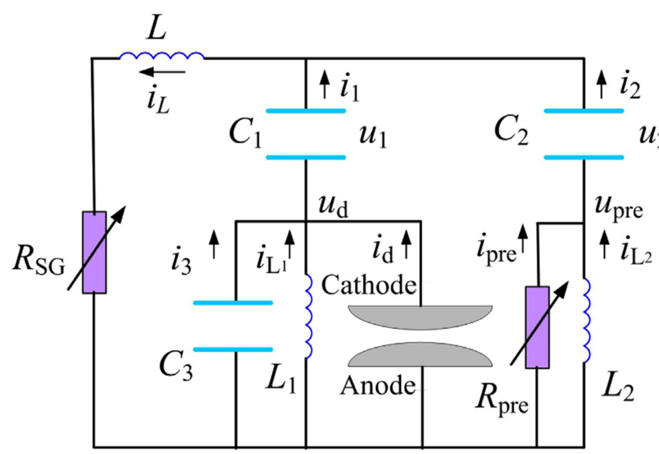

Fig. 3. Equivalent circuit diagram of LC inversion circuit.

$$\frac{di_{L1}}{dt} = \frac{u_d}{L_1} \quad (3)$$

$$\frac{di_{L2}}{dt} = \frac{u_d - u_1 + u_2}{L_2} \quad (4)$$

$$\frac{du_d}{dt} = \frac{i_L}{C_3} - \frac{i_{L2}}{C_3} - \frac{i_{L1}}{C_3} - \frac{i_d}{C_3} - \frac{u_d - u_1 + u_2}{R_{pre} \cdot C_3} \quad (5)$$

$$\frac{di_L}{dt} = \frac{u_1}{L} - \frac{i_L R_{SG}}{L} - \frac{u_d}{L} \quad (6)$$

u_1, u_2 and u_d are voltages of C_1, C_2 and main discharge respectively. i_{L1}, i_{L2} and i_L are branch currents of L_1, L_2 and L respectively. The variable resistance $R_{SG} = 0.1 + 100\exp(-t/(5 \times 10^{-9}))$ [12]. The main discharge current i_d can be expressed as follows:

$$i_d = e \cdot n_e \cdot u_e \cdot s \quad (7)$$

where e, s and u_e are electron charge, area of cathode and drift velocities of electron respectively. Based on the measuring result of quasi-stationary voltage, Apollonov gave a conclusion that only ionization of SF_6 by electron impact and electron attachment to SF_6 molecules are substantial processes for SSVD, at least for energy depositions not exceeding 200 J/l and SSVD durations longer than 200 ns (the deposited energy in unit time and unit volume is not exceeding 1 J/l/ns), whereas some influences can be neglected such as step ionization, Penning process, attachment of electron to excited molecules of SF_6, and ionization of dopes, etc. [13]. During the processes of SSVD in the SF_6-based gas mixtures, β_{ei} and k_d should be approximately equal, so their effect on electron concentration can be neglected in the simulation. Here, β_{ei} and k_d are rate constants of electron–ion recombination and electron-impact detachment of electrons from negative ions, respectively [14]. The continuity equation describing the growth of electron densities (n_e) between the electrodes is

$$\frac{dn_e}{dt} = n_e \cdot \alpha \cdot u_e - n_e \cdot \eta \cdot u_e + n_{pre}(t) \tag{8}$$

where α is collision ionization coefficient, η is adsorption coefficient, u_e is electron drift velocity and $n_{pre}(t)$ is the electron density produced by UV pre-ionization. Yoshiro has measured the electron density produced by single spark gap discharge, and found that the electron density was linear increase with the discharging current when the discharging current exceeded a threshold value [15]. Consequently, in the calculations $n_{pre}(t)$ is approximated by the form $n_{pre}(t)=k \cdot i_{pre}$, where k is constant coefficient (the value of k equals 1/e in the calculation) and the pre-discharging current $i_{pre}=(u_d-u_1+u_2)/R_{pre}$.

The specific expressions of the seven coupled differential equations are represented by Eqs. (1)–(6) and (8). Based on the Runge–Kutta theory, the seven variables (u_1, u_2, i_{L1}, i_{L2}, u_d, i_L, and n_e) can be obtained through solving the differential equations. The deposited energy can be expressed as the integral of main discharge voltage and current on time

$$W = \int_0^T i_d u_d \, dt \tag{9}$$

where T is the periodic time.

3. Comparison of numerical and experimental results

3.1. Numerical calculations

After charging to storage capacitance and before breakdown of SG switch, the terminal voltages of storage capacitances are equal to the voltage of HV and the currents of each branch circuits are equal to zero. These voltages and currents would be initial values of differential equations, for inductances and capacitances in the circuit limit the jump of currents and voltages respectively. The circuit parameters of non-chain pulsed DF laser and related data are shown in Table 1:

With the above initial values and related data, the differential equations was solved numerically using the Runge-Kutta method. Fig. 4 shows the calculations of main discharge voltage, current and pre-discharge voltage. Firstly, the terminal voltage of pre-ionization electrodes reaches its critical breakdown voltage (17 kV) rapidly, and spark discharge channel forms between the spark

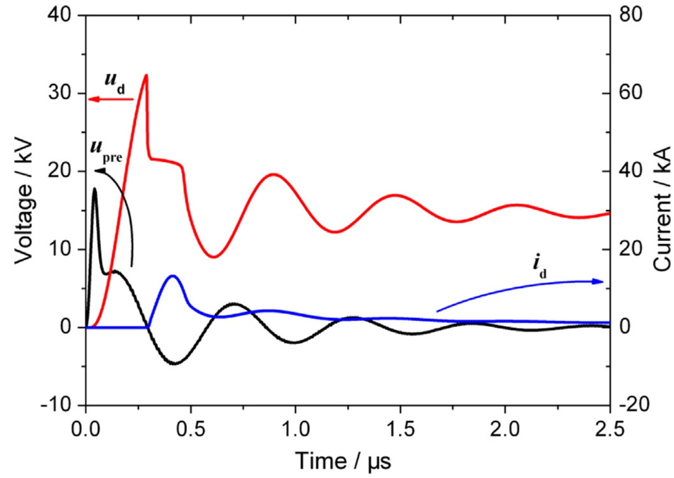

Fig. 4. Waveforms of main discharge voltage, current and pre-discharge voltage with DF laser.

pins. Then the pre-discharge voltage decreases to its sustaining voltage (7 kV), which can sustain spark discharge for 50 ns. After that, the pre-discharge voltage will attenuate to zero through the LC resonance. Secondly, after the breakdown of pre-ionization electrodes, through a delay time of 250 ns, the terminal voltage of main electrodes reaches its critical breakdown voltage (33 kV), realizing glow discharge breakdown. Then the main discharge voltage decreases to its sustaining voltage (21 kV) quickly, and this process of SSVD can continue 150 ns. Simultaneously with the breakdown of main discharge, the discharge current rises from zero and reaches peak value in the stage of SSVD. The deposited energy can be expressed as the integral of main discharge voltage and current on time, so the effective discharge is mainly concentrated on the stage of SSVD. From Eq. (9), we can obtain a deposited energy of 47.25 J. The total stored energy of the capacitance $W_0=0.5C_1u_0^2=131.206$ J, and the efficiency of deposited energy is 36.01%. The residual energy would be consumed by resistance elements in circuit.

3.2. Experimental results and discussion

The device of non-chain DF laser has been previously described in details [11]. The mixture ratio (SF_6:D_2) used in this experiment was 10:1, and the total pressure and charging voltage were equal to the values used in the calculations. Two high voltage probes of 60 kV were connected to the test points A and B (as shown in Fig. 1) in order to test voltage waveforms of main discharge and pre-discharge respectively. A room temperature HgCdTe detector was placed in the main optical path to test waveform of laser pulse. All these waveforms, just as shown in Fig. 5, were recorded by a TDS3052B oscilloscope with 500 MHz bandwidth. In Fig. 5, channel 1 is laser pulse shape of DF laser, channel 2 is the voltage waveform of pre-discharge which used a probe with attenuation

Table 1
Circuit parameters and related data of non-chain pulsed DF laser [16].

Parameters	Values	Parameters	Values
Working pressure p	10 kPa	Delay inductance L	2 μH
Area of cathode s	320 cm^2	Charging inductances L_1	600 μH
Gap of electrode d_1	4 cm	Charging inductances L_1	200 μH
Gap of spark pins d_2	5 mm	Number density of SF_6 N	$7.24 \times 10^{16} \times p/T$ cm^{-3}
Charging voltage u_0	34 kV	Collision ionization coefficient α/N	$11.269 \times (E/N)^{1.159}$
Main storage capacitances C_1	227 nF	Adsorption coefficient η/N	$7.0 \times 10^{21}\exp[-2.25 \times 10^{18}(E/N)]$
Pre-ionization capacitance C_2	52 nF	Drift velocities of electron u_e	$1.027 \times 10^{19} \times (E/N)^{0.7424}$
Peak capacitance C_3	30 nF	Electric field intensity E	u_d/d_1

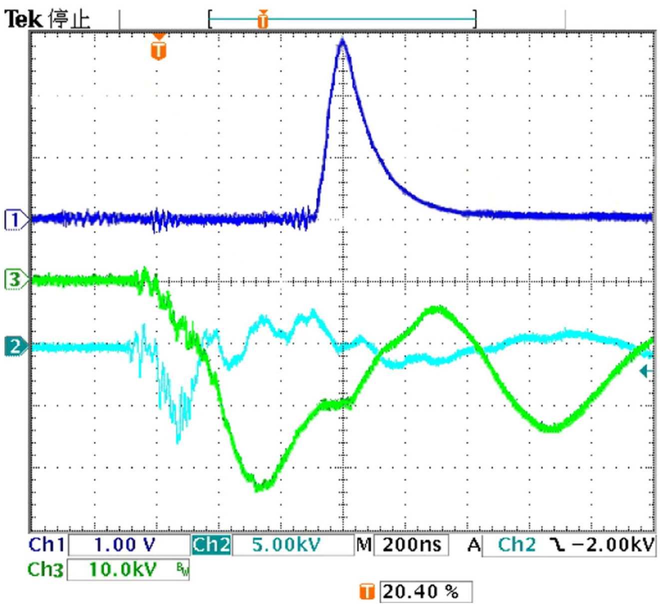

Fig. 5. Waveforms of discharge voltage and laser pulse: laser pulse shape (Channel 1), pre-discharge (Channel 2), main discharge (Channel 3).

ratio of 2000:1, so the voltage scale is 10 kV actually, and Channel 3 is the voltage waveform of main discharge which used a probe with attenuation ratio of 1000:1, so the corresponding voltage scale is 10 kV actually.

The breakdown voltage of pre-ionization electrodes is 15 kV, whose time of sustaining discharge is not obvious. After a delay time of 220 ns, the terminal voltage of main electrodes reaches its critical breakdown voltage (35 kV) and realizes glow discharge breakdown. Then the main discharge voltage decreases to its sustaining voltage (20 kV) quickly, whose process of SSVD can continue 100 ns. Lastly, the main discharge voltage damps to zero through the LC resonance slowly. With the breakdown of main electrodes, energy starts to inject into the gain area, which results in the dissociation of SF_6 molecules into F atoms and sub-fluoride molecules. Then F-atoms react with D_2 to generate excited DF molecules. Therefore the laser pulse starts to form with stimulated transition of excited DF molecules. The measured laser pulse width is about 148.8 ns, the single pulsed energy is 2.5 J, and the electrical to optical efficiency is 1.905%. The SSVD between main electrodes is shown in Fig. 6.

Comparing Fig. 4 with Fig. 5, the measured pre-ionization and main discharge voltage waveforms are consistent with the simulation results, and the start time of laser pulse in experiment matches that of deposited energy in calculation. The experimental sustaining stage of pre-ionization discharge waveform is not obvious. However the sustaining time of pre-ionization discharge is about 50 ns on calculation. The basic parameters (α, η, u_e, etc.) used for calculation neglected the influence of D_2 on discharge, which lead to low calculation of electron concentration, low current and longer life of plasma in the discharge area step by step. In addition, the occurrence of discharge instabilities may lead to shorten the sustaining time of discharge in the experiment. Therefore, the time of discharge sustaining on calculation is generally longer than experiment. In addition, the calculated sustaining time of main discharge voltage is 50 ns above the measured value, which may verify the difference of discharge sustaining time between calculation and experiment. To obtain accurate discharge duration, the results of calculation can be revised by minus 50 ns. Comparison of calculations and experimental results with discharge parameters are shown in Table 2. Revised calculations are consistent with experiments, thus this model can be applied to explore the discharge characteristics of non-chain DF laser.

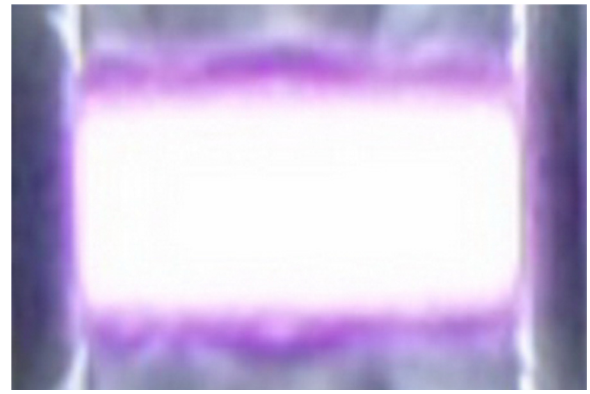

Fig. 6. Discharge photo between main electrodes.

Table 2
Comparison of calculations and experimental results with discharge parameters.

Comparing results	Calculations	Experimental result
Breakdown voltage of pre-ionization/kV	17	15
sustaining voltage of pre-ionization/kV	7	Not obvious
sustaining time of pre-ionization/ns	50	Not obvious
Breakdown voltage of main discharge/kV	33	35
sustaining voltage of main discharge/kV	21	20
sustaining time of main discharge/ns	150	100
Delay time/ns	250	220

4. Influence of circuit parameters on discharge

Using the above model, influences of delay inductance L and peaking capacitor C_3 on discharge were studied separately, whose results are shown in Figs. 7 and 8.

Theoretical calculation indicates that L has no effect on breakdown time and voltage of pre-ionization discharge. Therefore voltage waveform of pre-discharge is indicated by the dashed curve in Fig. 7(a) at $L=2$ μH to observe the delay time between main discharge and pre-discharge. The delay inductance has a great effect on voltage waveform of main discharge. The smaller the L, the steeper the pulse front of voltage waveform, and the shorter the delay time between pre-discharge and main discharge. Under the same condition of gas parameters, the delay inductance has no obvious effect on breakdown voltage, sustaining voltage and sustaining time of main discharge. As shown in Fig. 7(b), the delay inductance has obvious effect on the peak value of discharge current. According to the theory of gas discharge, the UV radiation produced by pre-ionization discharge can induce ionization of mixture gas. After the UV light starts to irradiate, the density of charged particles in discharge area will gradually increase till it reaches maximum. Then, because of the stop of UV radiation, ion–electron recombination, electron adsorption by SF_6, and some other effects, the density of charged particles will gradually decrease. When the density of charged particles reaches its maximum value, breakdown of main discharge may be most beneficial to form uniform glow discharge, and the discharge current is maximum under this condition. The calculated main parameters of discharge with different delay inductance are shown in Table 3.

Table 3 shows that when the delay inductance L equals 8 μH, the main discharge current reaches maximum 14.52 kA, the deposited energy in discharge area is upto 53.47 J, and the deposited efficiency is 40.753%, which are helpful to obtain a high output

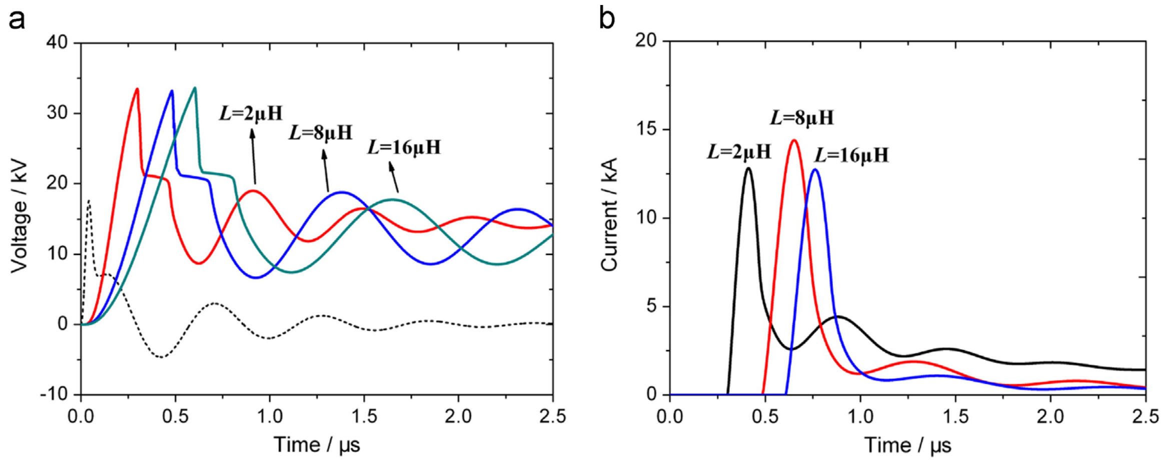

Fig. 7. voltage waveform (a) and current waveform (b) of *LC* inversion circuit at different *L*.

energy for DF laser.

The result in Fig. 8 shows that C_3 has obvious effect on discharge voltage and current. The smaller the C_3, the steeper the pulse front of voltage waveform, and the bigger the discharge current. Comparing the calculations of voltage and current at different values of C_3, it is found that a nonlinear relation existed between the sustaining time of discharge and C_3. When C_3=42 nF, the sustaining time of discharge is the longest, and the discharge current is moderate, which may be beneficial to deposit energy. When C_3=22 nF, the discharge current is bigger, but the sustaining time of discharge is smaller, which may cause instable discharge. The calculated main parameters of discharge with different peaking capacitor are shown in Table 4. The calculations show that when C_3=42 nF, the deposited energy is the biggest, which suggest that this peaking capacitor matches with the discharge parameters.

Table 3
Calculated main parameters of discharge with different delay inductance.

Delay inductance *L* (μH)	Delay time (ns)	Peak current (kA)	Deposited energy (J)	Deposited efficiency (%)
2	250	12.83	47.25	36.012
8	440	14.52	53.47	40.753
16	550	12.76	46.99	35.814

Table 4
Calculated main parameters of discharge with different peaking capacitor.

Peaking capacitor C_3 (nF)	Sustaining time (ns)	Peak current (kA)	Deposited energy (J)	Deposited efficiency (%)
22	135	16.94	48.02	36.599
42	155	15.56	50.65	38.603
62	142	12.95	38.62	29.435

5. Conclusions

A theoretical model of discharge for non-chain DF laser in a SF_6–D_2 gas mixture excited with UV pre-ionized electric-discharge is described. The discharge processes of non-chain DF laser are studied with this model and compared with experiment, and the model results of breakdown and sustaining time of discharge versus time showed good agreement with experiment data, which indicate that the model had good practicability. In addition to that, the influences of delay inductance and peaking capacitance on discharge characters are calculated, and conclusions are as follows:

(1) The delay time between pre-ionization and main discharge is determined by delay inductance, and the delay time that matches the discharge characters of gas mixture is helpful to deposit more energy.
(2) The peaking capacitance that matches the discharge parameters of LC circuit is helpful to increase the output

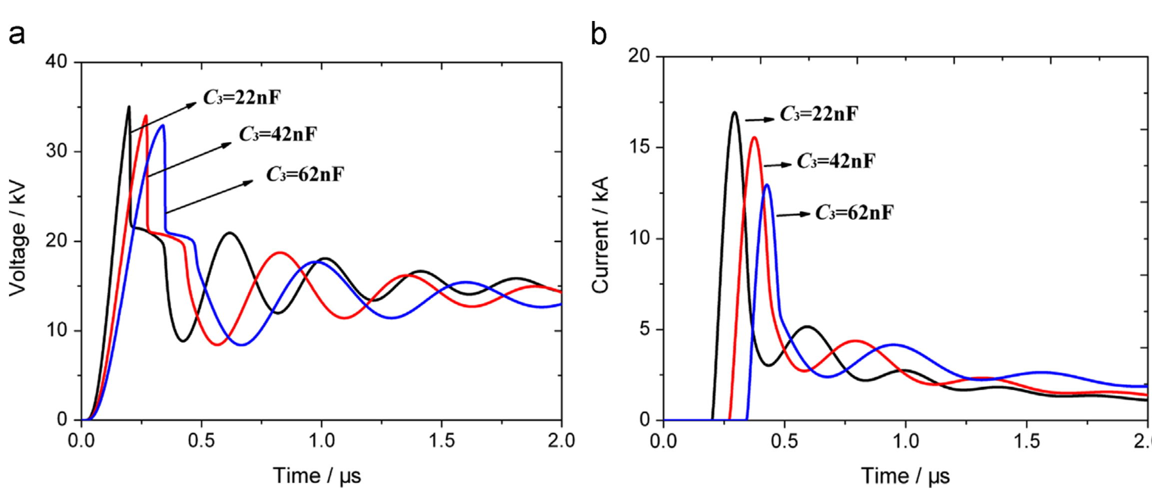

Fig. 8. Voltage waveform (a) and current waveform (b) of *LC* inversion circuit at different C_3.

performance of DF laser.

The model can effectively and conveniently describe the discharge processes of non-chain DF laser. The numerical calculation can show the evolvable relationship of discharge voltage and current with time intuitively.

Acknowledgments

This work is supported by the International Cooperation Special Fund from Ministry of Science and Technology, China PRC (No. 2011DFR10320).

Appendix A. Supplementary material

Supplementary data associated with this article can be found in the online version at http://dx.doi.org/10.1016/j.optcom.2015.11.004.

References

[1] V.Y. Agroskin, B.G. Bravy, Y.A. Chernyshev, S.A. Kashtanov, V.I. Kirianov, E. F. Makarov, V.G. Papin, S.A. Sotnichenko, G.K. Vasiliev, Aerosol sounding with a lidar system based on a DF laser, Appl. Phys. B 81 (2005) 1149–1154.
[2] B.I. Vasilev, O.M. Mannoun, IR differential-absorption lidars for ecological monitoring of the environment, Quantum Electron. 36 (2006) 801–820.
[3] G. Wilson, B.R. Graves, S.P. Patterson, R.H. Wank, Deuterium fluoride laser technology and demonstrators, Proc. SPIE 5414 (2004) 41–51.
[4] V.I. Lazarenko, S.D. Velikanov, I.N. Pegoev, S.N. Sinkov, Yu. N. Frolov, Analysis of DF laser applicability to SO_2 remote sensing in the atmosphere, Proc. SPIE 4168 (2001) 232–235.
[5] A.M. Razhev, D.S. Churkin, E.S. Kargapol'tsev, Chemical HF laser with pulsed inductive discharge initiation, Laser Phys. Lett. 10 (2013) 075002.
[6] Mainuddin, Gaurav Singhal, R.K. Tyagi, A.K. Maini, Development of safe infrared gas lasers, Opt. Laser Technol. 47 (2013) 56–63.
[7] A.A. Serafetinides, K.R. Rickwood, A.D. Papadopoulos, Performance studies of a novel design atmospheric pressure pulsed HF/DF laser, Appl. Phys. B 52 (1991) 46–54.
[8] N. Anderson, T. Bearpark, S.J. Scott, An X-ray preionised self-sustained discharge HF/DF laser, Appl. Phys. B 63 (1996) 565–573.
[9] H. Brunet, M. Mabru, F. Voignier, High energy-high average power pulsed HF/DF chemical laser, Proc. SPIE 2505 (1995) 388–392.
[10] V.V. Apollonov, K.N. Firsov, S.Y. Kazantsev, V.F. Oreshkin, A.V. Saifulin, Scaling up of non-chain HF (DF) laser initiated by self-sustained volume discharge, Proc.SPIE 3886 (2000) 370–381.
[11] P. Ruan, J.J. Xie, L.M. Zhang, J. Guo, G.L. Yang, D.J. Li, Q.K. Pan, G.J. Tan, F.J. Meng, Sh. M. Li, Computer modeling and experimental study of non-chain pulsed electric-discharge DF laser, Opt. Express 20 (2012) 28912–28922.
[12] G.N. Tsikrikas, A.A. Serafetinides, Discharge and circuit simulation of a plasma cathode TEA HF laser operating with a $He/SF_6/C_3H_8$ gas mixture, Opt. Commun. 134 (1997) 145–148.
[13] V.V. Apollonov, A.A. Belevtsev, K.N. Firsov, S. Yu Kazantsev, A.V. Saifulin, High power pulse and pulsed-periodic nonchain HF(DF) lasers, Proc. SPIE 4747 (2002) 31–43.
[14] A.A. Belevtsev, S.Y. Kazantsev, I.G. Kononov, K.N. Firsov, Detachment instability of self-sustained volume discharge in active media of non-chain HF(DF) lasers, Quantum Electron. 40 (2010) 484–489.
[15] Yoshiro Ohwadano, Tadashi Sekiguchi, Developtment and performance charachteristics of UV-preionized, high-power TEA pulsed CO_2 laser, Jpn. J. Appl. Phys. 19 (1980) 1493–1504.
[16] S.K. Dhali, A.K. Pal, Numerical simulation of streamers in SF_6, J. Appl. Phys. 63 (1988) 1355–1362.